



Hyperspectral Mapping for Soil and Crop Analysis

Hemalata V. Bhujle

Associate Professor, Department of Electronics and Communication Engineering, SDM College of Engineering & Technology, Dharwad, India

Abstract: In this paper, in the first part we discuss the approaches to performing reflective compensation for hyperspectral sensors. In the second part, we discuss the image fusion performance. These range from empirical techniques that rely to varying degrees to the radiative transfer theory developed. The radiative transfer solutions are made computationally efficient with simplifications and approximations. Approximations in case of model based approaches are based on adjacency effect assuming surface is Lambertian. Empirical methods they do not use model based approaches but they are developed and linked with radiative transfer formalism. In the paper we describe the results of hyperspectral fusion techniques also we conduct hyperspectral mapping for types of crop and soil analysis.

Keywords: Hyperspectral, Soil, Crop, fusion.

I. INTRODUCTION

There are various simplifications to the model based approaches. However there are some constraints to that. Also various model based approaches exist in atmospheric compensation/correction. Also in this section we carry out discussion on statistical analysis on hyperspectral and monochromatic images.

1.1 Simplification for Model-Based Approaches

There are two requirements for inversion. One being transmittances and spherical albedo for radiative transfer model and an additional method being atmospheric point spread functions. Water and aerosol that can be classified as variable species, size and vertical distribution would be used to generate a model of the at-aperture radiance as is done for vicarious calibration measurements. Atmospheric point spread function can be modelled with Monte Carlo simulation. Though Monte Carlo technique is computationally intensive it is applied on aerosol model with great accuracy and reasonable simplifications, such as computation for a limited number of angles and wavelengths followed by interpolation. Thus quantification of water and visibility can be addressed [1]. Water forms the droplets that scatter and condenses onto other aerosol particles which further changes their absorption and scattering properties, and hence influences transmission and visibility the adjacency effect is addressed through some approximations. First, surface is assumed to be Lambertian and the unknown BRDF is ignored. An estimate of the BRDF could be retrieved through iterations on the final solution if desired.

1.2 Model-Based Atmospheric Compensation

The visibility, water vapour and adjacency effect can be determined through appropriate equations. However compensation of the atmosphere can be summarized only through physics model. For that it is required to look at the look-up table in order to converge on the solution. Flow diagram for retrieving surface reflectance can be shown with Figure 2.1. In fig 2.1, we can see the retrieval of surface reflectance from calibrated radiance. Here the assumption is in regard of having adequate spectral coverage and resolution for radiance data. To determine cloudy pixels, a combination of brightness, band ratio and water vapour tests are required whereas, visibility, adjacency effect and phase function can be computed with a nominal aerosol model. However the distribution of aerosol distribution shouldn't be markedly different than standard aerosol types. In case the distributions are different then significant differences and errors may occur. The solution method to calculate the average surface reflectance involves computing a spatially averaged radiance image from which the spatially averaged reflectance is estimated [2].

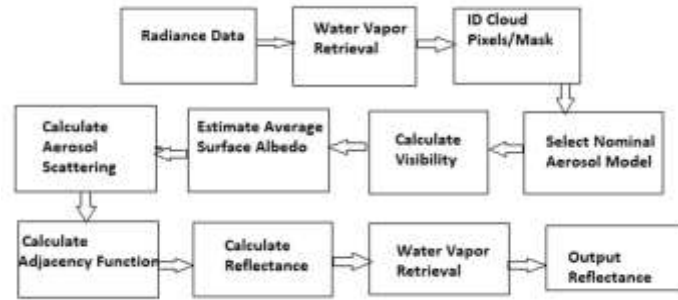


Fig 2.1 Flow diagram for atmospheric compensation.

1.3 Empirical atmospheric compensation

Empirical Line Method (ELM) is the primary approach for atmospheric compensation, as it assumes spectral reflectance of a clearly identifiable surface in the data. Here the quantity of reflected radiance is computed with the assumption of a scalar free atmosphere and the observed dark-subtracted response from the focal plane. Characteristic signature based other ELM approaches have been developed recently. Example for a characteristic signature based EM technique is the chlorophyll dominated reflectance technique in a highly vegetated environment [3].

1.4 Statistical analysis of Hyperspectral imaging data.

Hyperspectral imaging sensor organises data as a cube with two spatial and one spectral dimension where spectral dimension is given by at-sensor measured spectral dimension. Spectrum of a ground resolution is measured by the sensor which is provided by the value with coordinates (x,y) at a wavelength band centered at λ . Further, data can be viewed in the form of the collection of simultaneously taken images, at each spectral band or collection of spectra one for each ground resolution. Thus two image types are considered; one where scalar images in which each pixel has a singular value associated with it. Vector image is considered to be the second type of image where each pixel is considered to be the vector of values. Thus in the data exploitation knowledge of the distributional characteristics of hyperspectral images is important [4].

1.5 Statistical Analysis of Scalar (Monochromatic) Images

Histogram of an image is used for scalar image analysis. Histogram peaks are computed by finding pixels with minimum and maximum values that identifies theoretical distributions to model the data [5]. Figure 1.5 shows a scalar hyperspectral image and its histogram. From fig, we can find low contrast images which results due to the radiance values beyond 6000. But contrast can be increased by saturating all pixels beyond 6000 or by clipping all pixels above these values. The resulting results can be viewed in figure 1.5. According statistical analysis the data follow a particular commonly known as a normal distribution. The agreement between the distribution of the data and the theoretically expected distribution is evaluated visually using a probability plot.

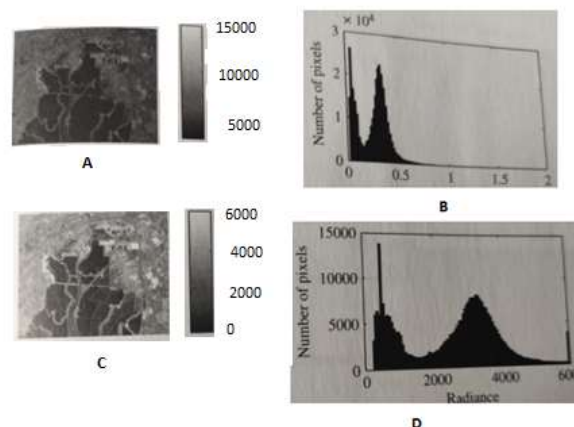


Fig 1.5. Illustration of scalar image histograms and their implications

II. HYPERSPECTRAL IMAGE FUSION

Image fusion systems are developed to gather all complementary information present in different images into a single image. The new image formed is suitable for human and machine interpretation. Also various image processing tasks such as segmentation, feature extraction and object detection can be carried out easily and efficiently with fusion technique. Also fusion systems help in dealing with massive data required in applications such as remote sensing, computer vision and environmental monitoring.

The proposed fusion technique relies on weight computation that depends on the local structures in the image. Further weight has been represented as a function of local structures in the image by subtracting smoothed image from the original image. Here each pixel value in the fused image is computed as normalized weighted average at its corresponding locations that results in separation of weak edges and fine structures. Here we have proposed fusion of remote sensing images with variable reflectance.

III. HYPERSPECTRAL MAPPING FOR SOIL AND CROP STUDY

Quality of the soil is an important factor for farmers to grow their crops. The type of crops cultivated depends on the pH and moisture content of the soil. Farmers usually do not perform soil testing as it consumes time and money. Hyperspectral mapping can be used to study the quality and crop types. The various features computed for soil include HSV histogram, auto correlogram, color moments, mean amplitude, energy and wavelet moments.

IV. RESULTS AND DISCUSSION**4.1 Hyperspectral Image Fusions:**

We tested the proposed method on various hyperspectral image sets and reported results on two sets. The purpose of fusion here is to form a single image by merging possible features from all the source images. For evaluating the proposed algorithm quantitatively, we use statistical measures like entropy, mean, variance and average gradient and vision perception for qualitative measure. We compare results of hyperspectral image fusion with (a) wavelet transform: we have used similar approach as proposed in [7] however; inputs are replaced with hyperspectral images, (b) contourlet transform used in [8] and (c) bilateral approach suggested in [6]. In this paper authors have considered HDR images, however we consider hyperspectral images. For NLM filter, we consider patch and search window size as 5 X 5 and 15 X 15, respectively. For bilateral method [6], patch size is considered as 5 X 5. All other parameters are chosen as suggested in the paper.

Table 4.1 Comparative results among different fusion approaches.

<i>Fusion method</i>	<i>mean</i>	<i>Std. dev.</i>	<i>entropy</i>	<i>gradient</i>
Hyperspectral Set-I				
Wavelet [46] method	83.21	19.76	5.58	4.51
Contourlet [47] method	86.34	20.13	5.61	4.73
Bilateral[43] method	88.37	21.93	5.86	5.31
Proposed method	88.10	22.13	5.91	5.53
Hyperspectral Set-II				
Wavelet [46] method	88.84	20.23	5.93	4.37
Contourlet [47] method	85.39	21.12	6.05	4.61
Bilateral[43] method	87.39	23.32	6.41	5.28
Proposed method	87.61	23.51	6.24	5.46

The constant M for the proposed method depends on the type of the images in the band and ranges between 40 to 60. Table.4.1.1 provides comparative results for various fusion techniques for hyperspectral image sets, respectively. From

the table, it is observed that the values obtained with wavelet transform [7] method are quite low. Better results are obtained with contourlet transform [8] in comparison with wavelet transform. The results obtained with bilateral method are better than the aforementioned methods. However, superior results are obtained with the proposed method for all quality measures, except slightly lower values for mean and entropy. Visual comparisons are shown in Fig 4.1.1. From these figures, we observe the superior results obtained with the proposed method compared to all.

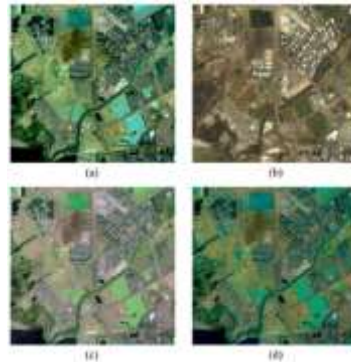


Fig.4.1 Visual comparison of the performance of various image fusion approaches over a block of the Moffett field hyperspectral image cube (Moffett02). Results of fusion using (a) the proposed method after the tristimulus display of fused images, (b) the wavelet approach, (c) the contourlet approach, and (d) the bilateral approach. Gamma is set to 1.5 for all color displays.

4.2 Hyperspectral Mapping for soil and crop Study

Disease identification of the vegetables can be done by using the images as shown in Fig 4.2. Images are preprocessed using image enhancement techniques such as contrast stretching to highlight the diseased portion from rest of the image. Further K means algorithm is used to segment diseased image portion from the rest. Precision can be increased by extracting boundary from the segmented images. Finally centroid is computed from the resultant image and image will be displayed.



Fig.4.2 Sample images of soil and crops

Soil quality can be measured by computing various features as illustrated in Table 4.2. For illustrative purpose, we show below mentioned features extracted for three soil samples namely humus clay, silty sand.

Table 4.2 Illustration of various features extracted from different soils.

Sl.no	Features	Humus clay	Sandy clay	Silty sand
1	HSV hist	0.0367	0.0291	0.045
2	Auto correlogram	0.06637	0.0793	0.063
3	Color moments	58.60	73.91	92.12
4	Mean amplitude	43.08	59.80	62.67
5	Energy	0.0192	0.0227	0.025
6	Wavelet Moments	3.226	4.353	4.536

**V. CONCLUSION**

In this paper, use of hyperspectral imaging for crop and soil image analysis is discussed. We analysed compensation techniques which are required for hyperspectral images. Hyperspectral images are fused to obtain a single image having all complementary information. We compared our fusion results with various other techniques. Images of diseased crops and computed various features of different soil to find its quality were also analysed.

ACKNOWLEDGMENT

The authors are grateful to Vision Group on Science and Technology (VGST) and Karnataka Science and Technology Promotion Society (KSTePS), Government of Karnataka for providing the funding and facilities to carry out this research work under KFIST-Level 1 Scheme with grant number: KSTePS/VGST/GRD-572/K-FIST (L1)/2020.

REFERENCES

- [1] Dimitris Manolakis, Ronald Lockwood and Thomas Cooley; Hyperspectral Imaging Remote Sensing, Cambridge University Press, 2016.
- [2] S.M.Kay Fundamentals of statistical Signal Processing; Estimation Theory, Volume I, Prentice Hall, New Jersey 1993
- [3] N.Keshava. A Survey of spectral unmixing algorithms. Lincoln Laboratory Journal, 14(1); 55-78,2003.
- [4] D. Lu et al. Change detection techniques. International Journal of Remote Sensing, 25(12): 2365-2401,2004
- [5] B.E. Saleh and M.C.Teich. Fundamentals of Photonics, 2 edition, Wiley series of Pure and Applied Optics. Wiley-Interscience, 2007.
- [6] W. Wang, P. Shui, and G. Song, "Multifocus image fusion in wavelet domain," in Intl. Conf. on Machine Learning and Cybernetics, vol. 5,2003, pp. 2887-2890.
- [7] S. Raman and S. Chaudhuri, "Bilateral filter based compositing for variable exposure photography," in Eurographics Conf., Munich, Germany, 2009.
- [8] A. Alejaily, I. Eirule, and M. Mangoud, "Fusion of remote sensing images using contourlet transform," in Intl. Conf. on Innovations and Advanced Technique in systems, Computing Sciences and Software Engineering, 2008, pp. 213-218.